Mon. Not. R. Astron. Soc. **000**, ??–?? (2012) Printed 30 April 2012 (MN LATEX style file v2.2)

Instrumentation Design of a Spatial FFT and FX Correlator for the BEST-2 Array

G. Foster[1], J. Hickish[1], D. Price[1], K. Zarb Adami[1]
[1] *Oxford University, Department of Physics*

30 April 2012

ABSTRACT
A spatial FFT imager and FX correlator has been developed using CASPER FPGA hardware for the BEST-2 array at the Radiotelescopi di Medicina in Italy. The spatial FFT imager takes advantage of BEST-2 as a regularly gridded array to produce a complete set of correlations for all unique baseline spacings by perform a 2D spatial FFT using $O(n \log n)$ operations. This is the first time a spatial FFT instrument has been used as a correlator on a radio telescope array. The FX correlator has been used to solve complex gain calibrations which are applied in the spatial FFT during observation. During the initial deployment of the instruments several bright radio sources were observed over multiple epochs. An analysis of the spatial FFT imager baseline and image quality is performed and compared to that of the FX correlator. Our study shows the spatial FFT data to be comparable in quality to the FX correlator. Further methods can be implemented in the real time calibration to improve the spatial FFT data quality.

1 INTRODUCTION

The Basic Element for SKA Training II (BEST-2) array is a subset of the Northern Cross cylindrical array, at the Radiotelescopi di Medicina in Italy. In this paper we present results from a new digital backend designed for this array, implemented on Field Programable Gate Array (FPGA) based hardware from the Collaboration for Astronomy Signal Processing and Electronics Research (CASPER[1]; Parsons et al. (2006)). The system developed provides fast-dump correlation, direct imaging, and beamforming capabilities.

The digital backend developed for BEST-2 comprises a 32 element digitizer and channeliser, a correlator, spatial Fast Fourier Transform (FFT) imager, and beamformer, implemented on ROACH[2] FPGA boards. Of particular interest is the spatial FFT imager which can produce a complete set of unique baselines using $O(n \log n)$ operations by taking advantage of the regularly gridded array geometry. The FX correlator computes all possible baseline pairs which scales as $O(n^2)$. Along with producing correlation data the spatial FFT functions as a gridded beamformer which has been used for pulsar observations. These instruments have been installed as prototypes for larger scale instruments currently in development. The correlator is being used to study the handling of large output data rates and the development of real time millisecond imaging using many antenna elements. The direct imaging system is being used to study the feasibility of such systems in arrays with regular geometric structure, as well as providing a platform for pulsar surveys and space-debris tracking capabilities with BEST-2. Since deployment, a number of sources with the correlator and imager have been successfully observed. Data have been reduced and calibrated using a combination of custom software and existing, popular radio synthesis imaging packages.

In the first section of this paper we give an overview of the BEST-2 Array, Sections 2.1, 2.2 and 2.3 cover a description of the channelization, correlation and image-domain processing system. Results from preliminary observations of bright radio sources from these systems are presented in section 3.1 and a comparison of data quality between the two instruments is presented in section **??**, with a discussion of results in section 4.

1.1 BEST-2 Array

The BEST-2 testbed at the Radiotelescopi di Medicina consists of 8 East-West oriented cylindrical concentrators, each with 64 dipole receivers critically sampling a focal line at 408MHz. Signals from these 64 dipoles are summed in groups of 16, resulting in 4 channels per cylinder, and a total of 32 effective receiving elements laid out on a *4-by-8* grid, shown in Figure 1.

BEST-2 was developed as a reliable, low cost frontend to be used in SKA development, with a core design requirement of simplicity in interfacing with different digital backends (Montebugnoli et al. 2009b). Extensive documentation of the development of the analogue chain developed for BEST-2 can be found in a number of papers (Perini (2009); Perini et al. (2009)). The top level specifications of the array are shown in Table 1.

[1] https://casper.berkeley.edu/
[2] Reconfigurable Open Architecture Computing Hardware – https://casper.berkeley.edu/wiki/ROACH

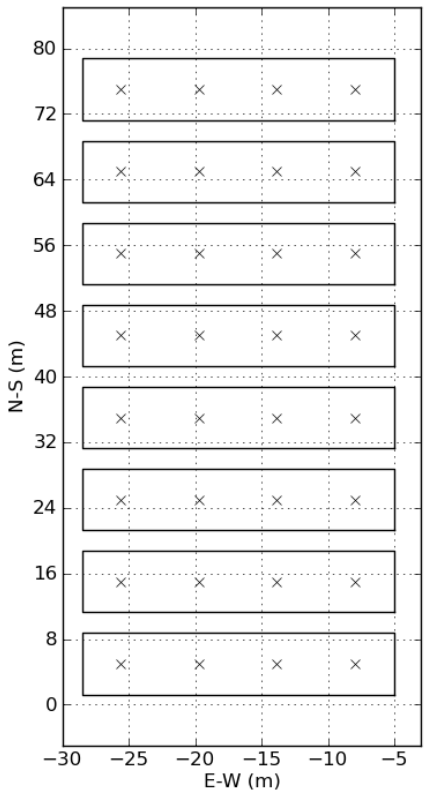

Figure 1. The 32 effective receiving elements of BEST-2, indicated by crosses, lie on a regular 4x8 grid. Each receiver is the analogue sum of 16 dipoles, critically spaced at 408 MHz in the East-West direction.

BEST-2 Array Specifications		
Array Properties		
Number of Cylinders	8	
Total Number of receivers	32	
Total Collecting Area	1411.2	m^2
A_{eff}/T_{sys}	11.65	m^2/K
Longest Baseline		
E-W	17.04	m
N-S	70.00	m
Bandpass		
Central Frequency	408	MHz
Analogue Bandwidth	16	MHz
Primary Beam		
Primary Beam Size	37.62	deg^2
Declination	5.7	deg
Right Ascension	6.6	deg
PSF		
PSF FWHM	0.9	deg^2
Declination	0.52	deg
Right ascension	1.73	deg

Table 1. The top level specifications of the BEST-2 Array, a subset of the collecting area of the Northern Cross, located in Medicina, Italy.

In 2008 the initial digital correlator backend of the array was based on iBOB and BEE2 FPGA boards from the CASPER group (Montebugnoli et al. 2009a). An upgraded digital backend has been developed using the ROACH board, also developed by CASPER, which includes an FX correlator, spatial FFT imager and beamformer.

2 INSTRUMENT DESIGN

An FX correlator and spatial FFT imager have been implemented in digital hardware for use with the BEST-2 array. Both instruments use the same digitization and channelization frontend. The hybrid design of the digital instruments make it possible to use both the correlator and imager concurrently. This allows a streamlined process for calibrating the spatial FFT imager, reduces the amount of hardware and allows for simultaneous observation with both instruments. The instruments have been implemented on ROACH boards which are a generic field programmable gate array (FPGA) board designed by CASPER for radio astronomy applications. The ROACH platform is based on a XILINX Virtex 5 SX95T[3] FPGA with interfaces to DRAM and QDR memory, high speed CX-4 connectors and a generic Z-DOK interface for connecting ADCs and various daughter boards, Figure 2. Additionally, the board has a PowerPC running BORPH, a variant of Debian Linux, which allows access to software registers and shared memory on the FPGA. Firmware is designed using MATLAB Simulink which is extended with XILINX DSP blocks and CASPER's open source DSP blocks[4]. Design specific DSP blocks and hardware interfaces have also created. Design models and control software are available from our project repository[5]. Instrument design specifications are presented in Table 2, further design detail is described in Sections 2.1, 2.2 and 2.3.

2.1 Digitization and Channelization

Signal digitization is performed using the Texas Instruments ADS5272 8 channel, 12 bit ADC. The ADC board, developed by Rick Raffanti[6], uses eight ADCs to channelize 64 streams at up to 65 Msps. In our design only 32 signal streams are digitized at 40 Msps which covers the 16 MHz analogue band. The ADC is clocked with a 160 MHz clock

[3] http://www.xilinx.com/support/documentation/virtex-5.htm
[4] https://casper.berkeley.edu/
[5] https://github.com/griffinfoster/medicina
[6] https://casper.berkeley.edu/wiki/64ADCx64-12

Digital Backend Specifications		
Digitizer/Channelizer (F-Engine)		
ADC Sampling Rate	40	Msps
ADC Sampling Precision	12	bit
Antenna-polarizations	32	single pol
PFB	4 tap FIR + 2048 point FFT	Radix-2 Biplex Real FFT
Quantization	4	bit
FX Correlator (X-Engine)		
Auto Correlations	32	
Cross Correlations	496	
Minimum Integration Length	6.55	ms
Output	10 GbE	SPEAD protocol
Spatial FFT Imager (S-Engine)		
2D FFT	8 x 16	
Beams	128	
Minimum Integration Length	1	s
Output	1 GbE	SPEAD protocol
Beamformer Output	10 GbE	Up to 8 Beams

Table 2. A three ROACH design where the correlator and spatial FFT imager use the same digitizer/channelizer frontend.

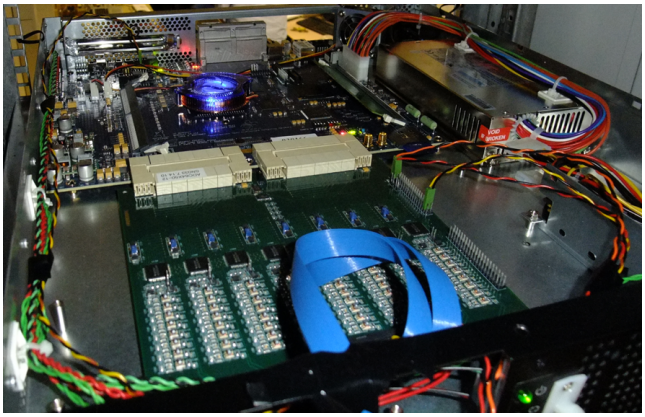

Figure 2. The 'F-engine' ROACH board, a Virtex 5 SX95T FPGA board, with the 64 input ADC connected via two Z-DOK connectors.

which is locked to a local maser source. During the analogue stage the radio frequency (RF) signal, centred at 408 MHz, is mixed down to baseband. Prior to digitization the last amplifier stage of the analogue chain has per signal adjustable gain useful for setting levels for optimum ADC quantization. This ADC is connected via a dual Z-DOK interface to an 'F-Engine' ROACH which performs the channelization. A block diagram of the design layout is shown in figure 3.

The ROACH board is clocked at four times the sample rate such that four signals are time division multiplexed onto a single stream. Channelization is performed with a four tap Hann filter, 2048 point polyphase filterbank (PFB) to produce 1024 samples per real antenna stream. The CASPER PFB has been modified to account for the signal multiplexing. Each channel has a width of 19.5 kHz and the output of the FFT stage is a 36 bit complex number. The narrow channel widths and PFB windowing allow for good frequency separation in the high RFI environment at the observatory. After channelization the samples are quantized down to 8 bit complex. An adjustable, per channel complex gain equalizer is used for amplitude and phase corrections before quantization. Complex gain calibration is essential to proper spatial FFT imaging and must be applied before the spatial FFT. The FX correlator is used to generate calibration coefficients which are applied back into the equalizers. A selectable mux is available to skip the phase coefficients on the FX correlator data stream. Post equalization, the data stream is split in two for specific reordering for the correlator and imager. The correlator data stream is reordered to 128 time samples for a single antenna for a single frequency channelr, followed by the next antenna and cycles back onto the next frequency channel. The imager takes in one time sample of each antenna for a given frequency channel and cycles through 128 time samples before stepping to the next frequency channel. After data reordering each stream is sent over high speed XAUI at a rate of 5.12 Gbps to the correlator and imaging boards. The FPGA resource usage is listed in Table **??**. There are sufficient resources to include additional features in the 'F-Engine', including, for example, finer channelization, an increase in antennas or an increase in bandwidth.

2.2 FX Correlator

An FX correlator design is a standard design for large bandwidth and many antenna arrays. The F component represents the frequency channelization, and the X is a complex multiply and accumulate (CMAC). An overview of the architecture is presented in Romney (1999). Architecture efficiency goes as $O(M\log M) + O(N^2)$ where M is the number

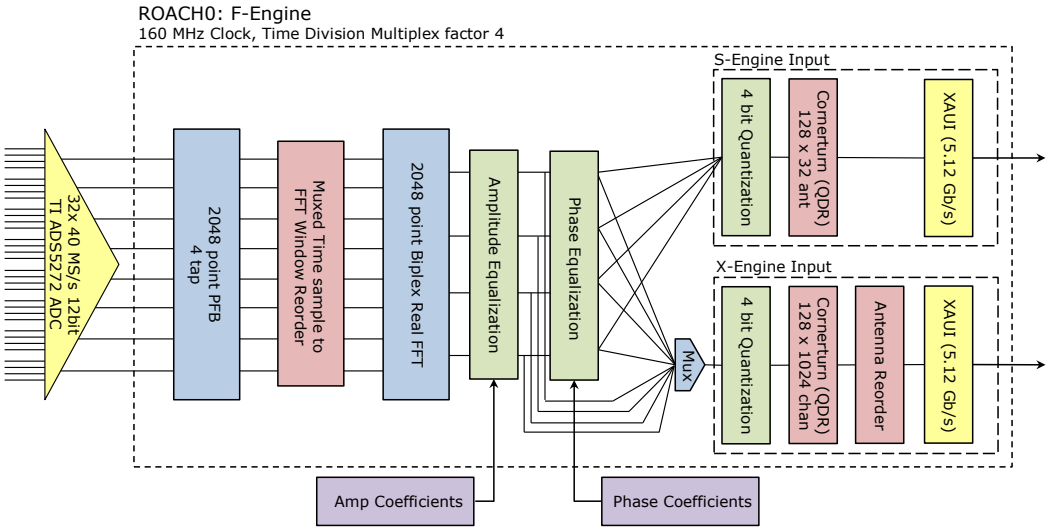

Figure 3. During observations amplitude and phase coefficients are applied to scale the power for the 4 bit correlation and apply phase corrections for the spatial FFT.

of FFT frequency channels and N is the number of antenna-polarizations. The core component to the X stage of the FX correlator is the complex multiplication of all pairs of independent signals for each frequency channel. A pipelined x-engine, based on the general CASPER block originally designed by Lynn Urry(Urry et al. 2007), is used for multiplier efficiency. The pipeline design is constructed out of $M/2$ 'taps' where the i^{th} tap computes the correlation between antennas A_j and A_{j+i} for every antenna A_j of M total antennas. To maximize the multiplier usage a loopback is added to use every i^{th} tap to compute the correlation of antennas A_j and $A_{M/2+j+i}$, fig. **??**. Each tap accumulates for t time samples to reduce the output data rate.

An asynchronous architecture is used between the f-enigne and x-engine boards. The x-engine board has been clocked to 200 MHz, well above the 160 MHz f-engine board, this assures the x-engine board will never have input buffer overflows during the windowing stage. The XAUI interboard connection is a streaming interface which guarantees the same output order as input order but with variable latency. In rare cases the XAUI interface can drop 64 bit words during the streaming, this requires an initial stage to track the number of words received between headers. In case of missing words the entire payload is dropped and counters reset for the next header. A correlation is only performed on a per channel basis. The channelized band can be split up into portions and processed in parallel across multiple x-engines. This allows a larger bandwidth to be processed at the cost of increased logic and multiplier resource utilization. We currently under utilize the available resources on the FPGA, table **??**. For this design two pipelined x-engines are used which each processes half of the band, figure 5.

The x-engine design requires a continuous stream of data for 128 samples of all antennas for a single frequency channel. Prior to the x-engine, samples are buffered up into windows to guarantee valid data during a cycle of the x-engine. For reasons related to the design the 32 single polarization signals are treated as 16 dual polarization signals. This causes a small number of redundant baseline correlations and a conjugation effect which is corrected in post processing. During the x-engine stage an initial accumulation of 128 sample is performed after the complex multiply to reduce the output rate to roughly the input rate. This limits the minimum integration time to 6.55 ms. In addition to the standard CASPER pipelined x-engine design an optimized version has been tested. This new optimized design efficiently uses the full bit width of the Xilinx DSP48 multipliers to reduce the total multiplier usage by a 75%. A description of this optimized design is in preparation.

A vector accumulator using the on board QDR memory is used for longer integration lengths. This second accumulator is software controlled with integration lengths ranging from milliseconds to minutes. A completed integration is sent to a receive computer over a 10 GbE connection. Integrations are packetized using the SPEAD protocol[7] and transmitted over UDP.

2.3 Spatial FFT

When N receiving elements in an antenna array are placed on a regularly spaced grid, a well known method for producing a complete set of orthogonal beams on the sky is the spatial fast Fourier transform (Williams 1968). Such a beamforming implementation will generate N beams on the sky, with a computational cost of $O(N \log N)$. For large arrays, where many beams are desired, this can be a significant computational saving, with the alternative, so-called *DFT beamforming*, requiring $O(N)$ operations per synthesized beam. To date, the largest such astronomical implementation of such a spatial fast Fourier transform beamformer is the 64 element dish array constructed in 1994 at Waseda University, Japan (Otobe et al. 1994).

More recently, spatial FFT based processing has been

[7] https://github.com/ska-sa/PySPEAD

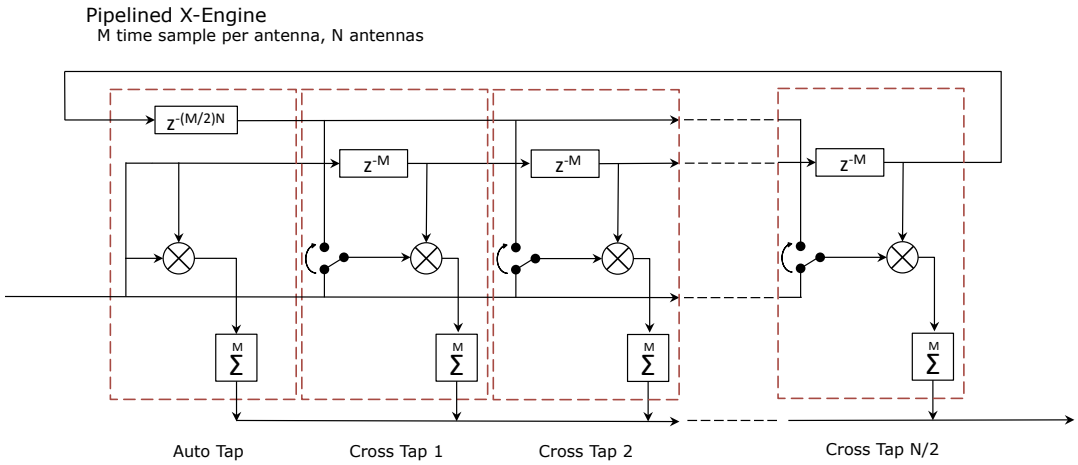

Figure 4. The input is ordered as M time samples per antenna per frequency channel. An accumulation stage after the complex multiply reduces the data rate of each tap. Outputs are multiplexed onto the same output using a valid signal.

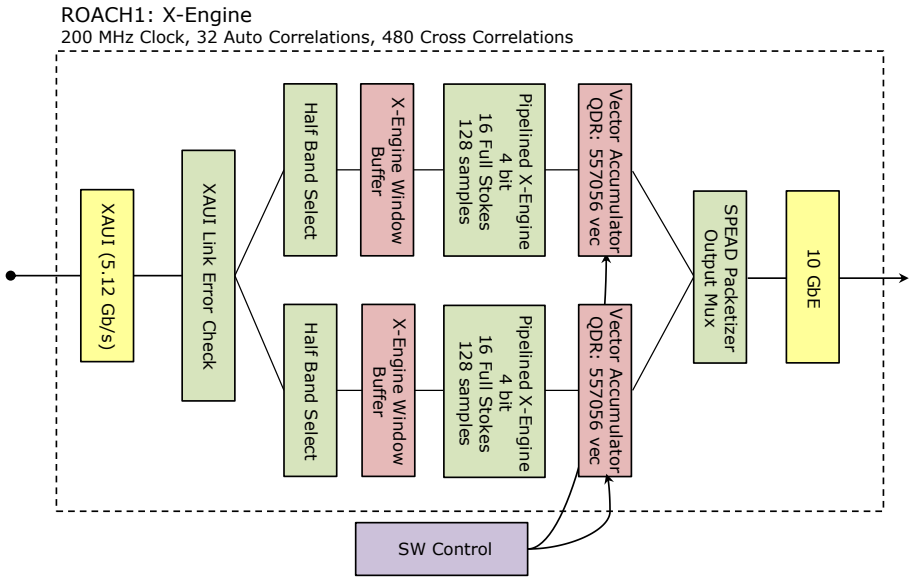

Figure 5. Two parallel pipelined x-engines are used, each processes half of the band.

revisited in the literature with an emphasis on the correlation matrix, rather than the collection of beams, as the mathematical object of interest (Tegmark & Zaldarriaga 2009) (Tegmark & Zaldarriaga 2010). In the method outlined by Tegmark & Zaldarriaga, zero padding is applied to the matrix of antenna signals before the spatial FFT is performed, and as such, the complete set of visibilities for all unique baselines in the array can be obtained, post integration, by inverse Fourier transform. Conversely, in the image plane, the zero-padding required by the prescribed algorithm results in the generation of $2^m N$ beams on the sky and is dependent on the number of dimensions, m, in the antenna array. Regardless of potential downstream visibility domain processing, this oversampling of the sky by a factor 2^m has the benefit of increasing the instantaneous uniformity of sky coverage by synthesized beams, which somewhat alleviates the limitations associated with the inability to steer multiple beams independently.

In the BEST-2 backend described here, the requirements on the spatial FFT processor were multifold. Firstly, the system should be capable of generating images on an O(second) timescale, by the method described by (Tegmark & Zaldarriaga 2009). Further, the system should be capable of passing formed beams at full bandwidth, i.e. without any accumulation, to downstream time domain processing systems such as the real-time pulsar dedispersion engine (Magro et al. 2011).

This redundancy for the BEST-2 array is show in Figure 6. Instead of making individual correlations of the same baseline as in an FX correlator the correlation of the average of each baseline can be computed. This optimization relies on the assumption that each redundant baseline measurement is indeed identical. Thus any calibration to the complex gains must be applied before the spatial FFT.

Though the X-Engine and S-Engine use the same F-Engine each requires a unique data windowing order. For

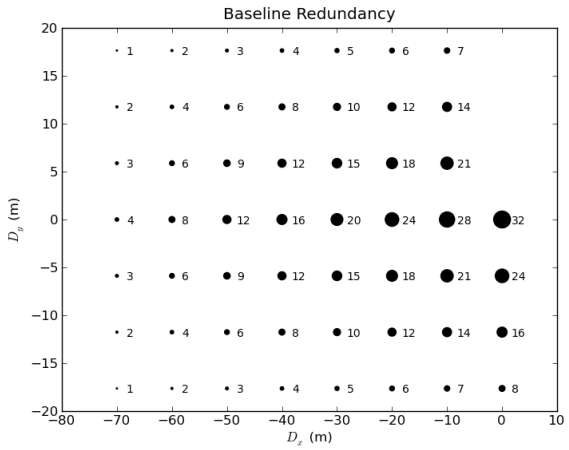

Figure 6. A 4 by 8 regularly gridded array has 53 unique baselines, 480 cross correlations are performed. The number of redundant baseline measurements is labelled and represented by the size of each circle.

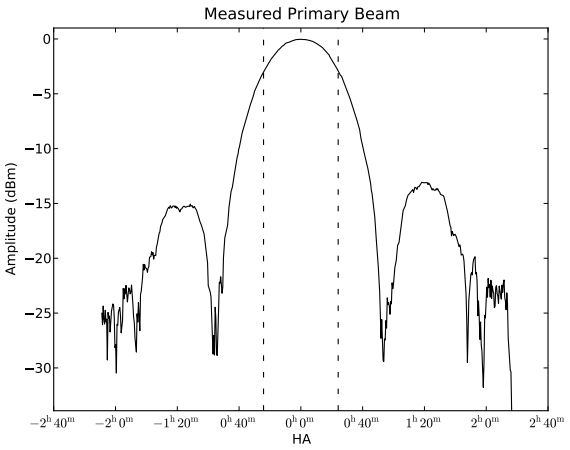

Figure 8. A measured east-west primary beam based on the correlation between antennas 1N-6-1 and 1N-1-3, which are representative of typical antennas, based on a Cassiopeia A transit. The dashed lines indicate the FWHM points. The antennas have a sinc response to a point source, as expected. The first sidelobes are -15 dB down from the peak.

the S-Engine a window is made up of N antennas by M time samples for a given frequency channel. A similar XAUI interface and windowing scheme is used as in the X-Engine which buffers up windows of valid data to stream into the spatial transform. The 2D spatial transform is performed using an 8 point FFT followed by a cornerturn and 16 point FFT. A block diagram of the design layout is shown in figure 7. The BEST-2 array is a grid of 4 by 8 antennas, the data is zero padded before input into the 8 by 16 point spatial transform. A 4 by 8 point spatial transform will only produce gain information for each spatial position, which can be interpreted as an array of beamformers covering the field of view. This zero padding is necessary to produce both the gain and phase information of each spatial position which is an effective baseline. Each effective baseline is an average of all possible baselines with the same spatial dimensions. The four fold increase is the number of outputs from the spatial transform by double padding introduces a number of redundant calculations. The spatial transform produces 128 outputs. There are only 53 unique baselines in a 4 by 8 grid. The datarate out of the S-Engine is reduced by a two stage vector accumulator. A fixed 128 sample vector accumulator reduces the output of the second stage FFT so that the 1024 channels of the 128 computed spatial components can be multiplexed onto one line and accumulated in a software controllable QDR vector accumulator. Accumulations are sent out over the 1 GbE PowerPC interface using the a SPEAD UDP packet format. Individual beams can be selected out before accumulation and sent over 10 GbE in a LOFAR beam packet format which is used for pulsar processing.

3 DEPLOYMENT AND INITIAL OBSERVATIONS

Instrumentation was installed and tested during March 2012, during which time various bright radio sources were observed. Since the Northern Cross is a transiting array there is a limited period of time each day in which a source is in the primary beam. Bright sources such as Cygnus A, Cassiopeia A and Taurus A along with a number of 3C sources were observed along with multiple constant declination 24 hour cycles.

Raw data from the correlator and imager is recorded to HDF5 files using a SPEAD protocol receive script. A suite of python scripts have been written to interface and manipulate the data in this pre-calibration stage. A python FITS-IDI package has been written to convert HDF5 files into the standard FITS format which can be read by AIPS and CASA[8]. This allows for conversion to the Measurement Set format which most packages can interface with.

3.1 FX Correlator Imaging

The East-West full width half max (FWHM) beam size of an individual element is $\approx 11.25^\circ$ which translates to a 45 minute 'observation time' for a source, as seen in the measured primary beam, figure 8. For the the bright A class sources this time can be extended since they remain the dominating source well after crossing the FWHM. Observations of 80-90 minutes are possible which gives an small improvement in uv coverage at the cost of properly accounting for the amplitude modulation due to the primary beam. This warrants a small sensitivity benefit for a large calibration cost. Most images are created using data within a few minutes of the source transit time. The high sidelobes in the primary beam, figure 8, cause the bright class A sources to dominate even when they are far from the field of view and makes it difficult to perform calibration and imaging near these sources.

[8] https://github.com/telegraphic/pyfitsidi

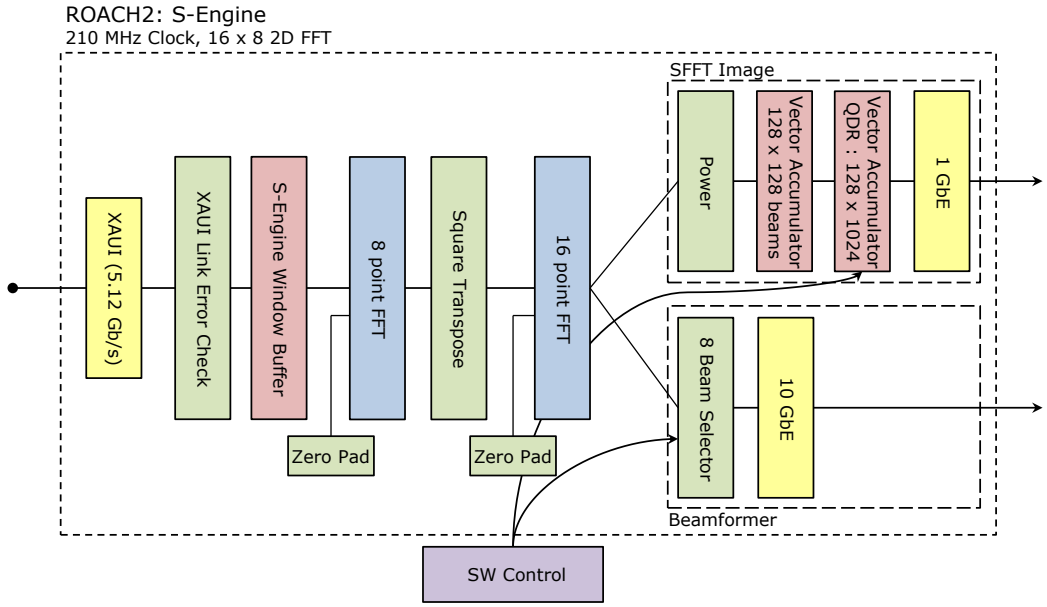

Figure 7. During the two stage spatial FFT the streams are zero padded to provide phase information of each baseline.

4 CONCLUSION

An FX correlator and spatial FFT imager have been successfully installed on the BEST-2 array at Medicina Observatory. The digital firmware was developed using the open source CASPER libraries and their generic ROACH hardware. This is the first time a spatial FFT imager has been used to produce complex baseline correlations. Both instruments can operate simulatenously which has allowed us to compare the respective data quality.

We have shown that the spatial FFT imager produces correlations similar to that of a traditional FX correlator. Complex gains are derived from calibration sources and applied during observations. The FX correlator data can be improved with further self calibration. Self calibration can not be performed on the spatial FFT imager since the effective baseline is a linear combination of redundant spacing baselines. The BEST-2 array is limiting our ability to improve the calibration. Bright sources are needed in the field of view to derive calibrations. A more advanced calibration method which can take into account multiple sources would allow more fields to be used for calibration and improve the time difference between calibration observation and science observation.

For low frequency dipole arrays which have a very large field of view there will always be bright sources in the field to calibrate against. With a fast enough calibration algorithm a small correlator can be used to derive gains on short timescales $O(seconds)$ and apply them to the spatial FFT imager. A good sky model and close time proximity between calibration observations and science observations will bring the spatial FFT calibration closer quality to a FX self calibration result.

With the successful installation and testing with the spatial FFT imager on the BEST-2 array we are working on developing the system further for science observations. Medicina Observatory is involved with space debris tracking using BEST-2 in a beamformer mode. The spatial FFT provides all beams within the field of view. This would improve the ability to detect and track space debris with the array. As noted earlier the beams have been used with a dedispersion machine to detect various pulsars. Work on this is in further development.

REFERENCES

Magro A., Karastergiou A., Salvini S., Mort B., Dulwich F., Zarb Adami K., 2011, MNRAS, 417, 2642

Montebugnoli S., Bartolini M., Bianchi G., Naldi G., Manley J., Parsons A., 2009a, in Proceedings of Wide Field Astronomy & Technology for the Square Kilometre Array (SKADS 2009). 4-6 November 2009. Chateau de Limelette, Belgium, pp. 355–358

Montebugnoli S., Bianchi G., Monari J., Naldi G., Perini F., Schiaffino M., 2009b, in Proceedings of Wide Field Astronomy & Technology for the Square Kilometre Array (SKADS 2009). 4-6 November 2009. Chateau de Limelette, Belgium, pp. 331–336

Otobe E. et al., 1994, Publications of the Astronomical Society of Japan, 46, 503

Parsons A. et al., 2006, in Asilomar Conference on Signals and Systems, Pacific Grove, CA, pp. 2031–2035

Perini F., 2009, in Proceedings of Wide Field Astronomy & Technology for the Square Kilometre Array (SKADS 2009). 4-6 November 2009. Chateau de Limelette, Belgium., pp. 341–345

Perini F., Bianchi G., Schiaffino M., Monari J., 2009, in Proceedings of Wide Field Astronomy & Technology for the Square Kilometre Array (SKADS 2009). 4-6 November 2009. Chateau de Limelette, Belgium, pp. 351–354

Romney J. D., 1999, in Astronomical Society of the Pacific Conference Series, Vol. 180, Synthesis Imaging in Radio

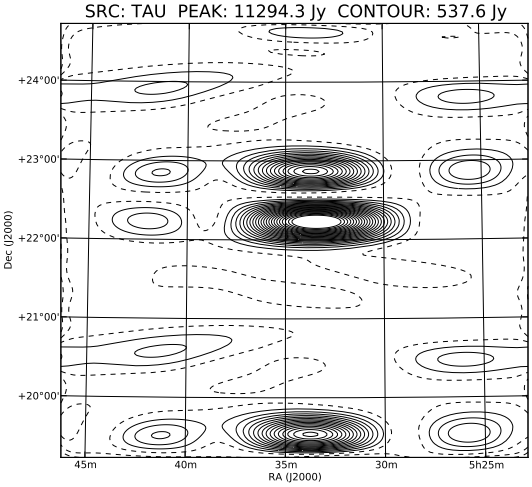

(a) Uncalibrated image of Taurus A.

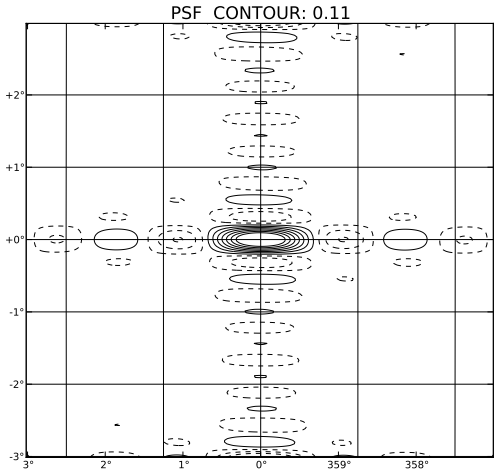

(b) Point spread function. The high, regular sidelobes are an effect of the regularly gridded array.

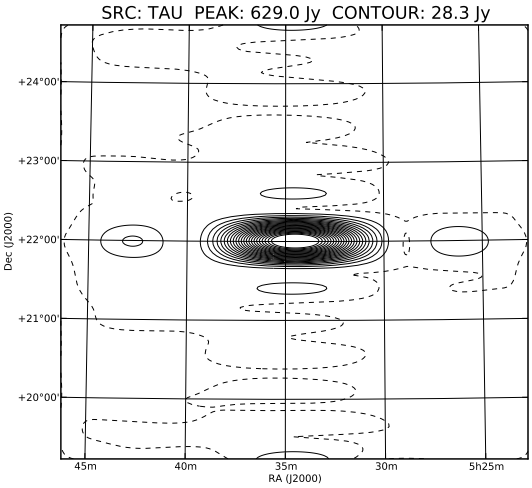

(c) Dirty image formed, using natural weighting, after applying complex gain solutions. The structure from the PSF is clearly visible. The dynamic range of this image is ~ 150.

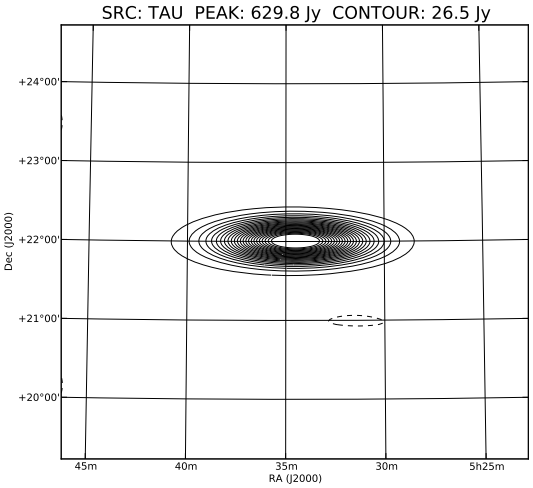

(d) Cleaned image of the field, Taurus A is the dominating point source with a peak of 730 Jy, the image have a dynamic range of ~ 350.

Figure 9. Images and PSF formed from an FX correlator two minute snapshot observation of Taurus A.

Astronomy II, G. B. Taylor, C. L. Carilli, & R. A. Perley, ed., p. 57

Tegmark M., Zaldarriaga M., 2009, Phys. Rev. D, 79, 083530

Tegmark M., Zaldarriaga M., 2010, Phys. Rev. D, 82, 103501

Urry W., Wright M., Dexter M., MacMahon D., 2007, ATA Memo: The ATA Correlator. Tech. Rep. 73, University of California, Berkeley

Williams J. R., 1968, The Journal of the Acoustical Society of America, 44, 1454

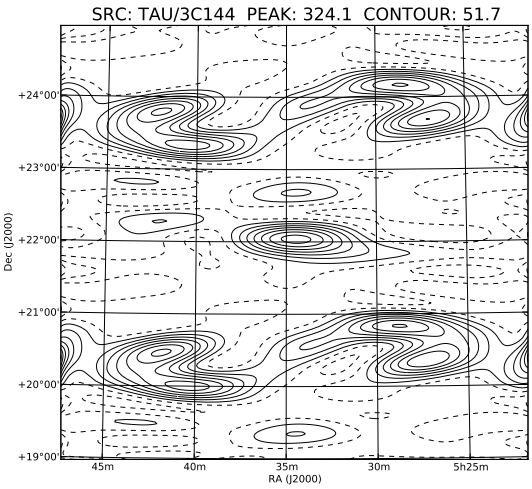

(a) Dirty image of Tau/3c144 formed before applying complex gain calibrations in the F-Engine for the spatial FFT. The uncalibrated phases spread the power through out the image.

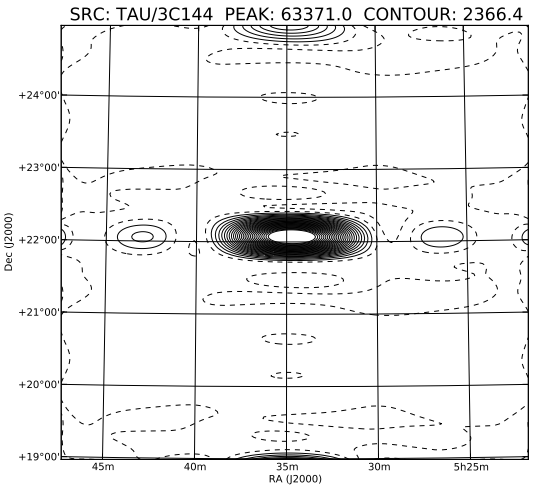

(b) Dirty image of Tau/3c144 with complex gain calibrations applied. This image has a signal to noise ratio around 100, a standard CLEAN method can be used to improve the image dynamic range.

Figure 10. After applying complex gain calibration a bright point source such as Tau/3c144 appears similar to the array PSF, and has a significant improvement in the image fidelity compared to the uncalibrated image.